Applied Surface Science 255 (2009) 6968–6977

Contents lists available at ScienceDirect

Applied Surface Science

journal homepage: www.elsevier.com/locate/apsusc

Corrosion protection of Mg/Al alloys by thermal sprayed aluminium coatings

A. Pardo [a,*], P. Casajús [a], M. Mohedano [a], A.E. Coy [a], F. Viejo [a], B. Torres [b], E. Matykina [c]

[a] Departamento de Ciencia de Materiales, Facultad de Químicas, Universidad Complutense, 28040 Madrid, Spain
[b] Departamento de Ciencia e Ingeniería de Materiales, ESCET, Universidad Rey Juan Carlos, 28933 Móstoles, Madrid, Spain
[c] Corrosion and Protection Centre, School of Materials, The University of Manchester, P.O. Box 88, Sackville Street, Manchester M60 1QD, United Kingdom

ARTICLE INFO

Article history:
Received 12 January 2009
Received in revised form 5 March 2009
Accepted 6 March 2009
Available online 17 March 2009

Keywords:
Magnesium
Aluminium coatings
Corrosion
Thermal spraying

ABSTRACT

The protective features of thermal sprayed Al-coatings applied on AZ31, AZ80 and AZ91D magnesium/aluminium alloys were evaluated in 3.5 wt.% NaCl solution by electrochemical and gravimetric measurements. The changes in the morphology and corrosion behaviour of the Al-coatings induced by a cold-pressing post-treatment were also examined. The specimens were characterized by scanning electron microscopy, energy dispersive X-ray analysis and low-angle X-ray diffraction. The as-sprayed Al-coatings revealed a high degree of porosity and poor corrosion protection, which resulted in galvanic acceleration of the corrosion of the magnesium substrates. The application of a cold-pressing post-treatment produced more compact Al-coatings with better bonding at the substrate/coating interface and higher corrosion resistance regardless of the nature of the magnesium alloy.

1. Introduction

Magnesium alloys are promising materials in the automotive industry where their lightweight can be used to great advantage and contribute to energy savings and reduced environmental impact [1]. However, the use of magnesium alloys is limited by their low corrosion and wear resistance [2,3]. Thus, the corrosion protection of magnesium alloys has evoked great interest during recent years. Several surface treatments such as anodising, chemical conversion, gas-phase deposition processes and electroplating can be used for tailoring the surface properties of magnesium alloys [4–6].

Among gas-phase deposition processes, thermal spraying (TS) technology offers a variety of techniques that allow the deposition of a wide range of functional coatings designed for specific environments [7–9]. For instance, TS processing is widely used in the automotive industry to produce coatings on transmission and engine parts such as synchronizing rings, shift forks and large volume of piston rings [10,11]. Recent studies have also shown that thermal spraying has a high potential for surface modification of magnesium alloys [12–20].

Regarding Al-coatings, they can be deposited on magnesium alloys using several routes [21,22]. For instance, Al-rich coatings can be obtained by painting and further heating at ~400 °C [23,24]. Even thought the coatings were not very uniform, the formation of the $Mg_{17}Al_{12}$ phase improved the hardness and corrosion resistance of the magnesium alloy. This approach is in line with the fact that aluminium produces a significant improvement of the corrosion resistance of Mg/Al systems by formation of aluminium rich oxides as well as networks of β-phase ($Mg_{17}Al_{12}$) [25,26].

In the case of aluminium-based thermal sprayed coatings applied to magnesium alloys [12,16,18–20] and the assessment of their corrosion behaviour [16,18,19] the number of studies is relatively scarce. In general, the coatings produced by TS process are quite uniform in thickness and they do not exhibit phase transformations with respect to the original powder, which is advantageous for achievement of certain control over desirable properties, *i.e.* corrosion resistance. Although the Al-TS coatings may present interfacial reactions with the magnesium surface during the process, the composition of the coating can be controlled by heat post-treatments [19,20]. And in the case of high levels of porosity the coatings can be consolidated by several post-treatment methods [16].

In the present study, the corrosion behaviour of Al-TS coatings deposited on three commercial magnesium/aluminium alloys—AZ31, AZ80 and AZ91D—was evaluated in 3.5 wt.% NaCl. The effect of a cold-pressing post-treatment on the morphology and corrosion performance of the coatings was also investigated.

2. Experimental

2.1. Test materials

Chemical compositions of the tested magnesium alloys (AZ31, AZ80 and AZ91D) are listed in Table 1. Pure Mg was used as the reference material. Mg and AZ31 were fabricated in wrought condition and supplied in plates of 3 mm thickness, whereas AZ80

* Corresponding author. Tel.: +34 1 3944348; fax: +34 1 3944357.
E-mail address: anpardo@quim.ucm.es (A. Pardo).

0169-4332/$ – see front matter © 2009 Elsevier B.V. All rights reserved.
doi:10.1016/j.apsusc.2009.03.022

Table 1
Nominal composition of the materials tested.

Material	Elements (wt.%)									
	Al	Zn	Mn	Si	Cu	Fe	Ni	Ca	Zr	Others
Mg	0.006	0.014	0.03	0.019	0.001	0.004	<0.001			
AZ31	3.1	0.73	0.25	0.02	<0.001	0.005	<0.001	<0.01	<0.001	<0.30
AZ80	8.2	0.46	0.13	0.01	<0.001	0.004				<0.30
AZ91D	8.8	0.68	0.30	0.01	<0.001	0.004	<0.008			<0.30

and AZ91D alloys were manufactured by casting using for the experiments billets of 300 mm × 10 mm and 250 mm × 10 mm, respectively. All the materials were supplied by Magnesium Elektron Ltd.

2.2. Thermal sprayed aluminium coatings

Prior to TS process, the alloy surfaces were sandblasted with corundum particles (1 mm diameter) in order to enhance the adhesion of the deposited coatings. Al-coatings were applied using aluminium powder with an average particle size of 125 μm (Castolin, 99.5% Al) and a flame spray gun (Castolin DS8000 system with a SSM40 modulus), which provides a thermal power of 28 kW. The following main processing parameters were used: spraying distance of 20 cm; neutral flame (*i.e.* balanced amounts of oxygen and acetylene to get full combustion) and a transversal gun displacement over the sample surface of 150 cm min^{-1}; material feeding rate of ~1.0 g s^{-1} and average particle speed of 300 m s^{-1}. In order to reduce the level of porosity in the coatings, a cold-pressing post-treatment was carried out at a pressure of 32 MPa for 3 min at room temperature.

2.3. Microstructural characterization

For metallographic characterization of the coated specimens, cross-sections were wet ground through successive grades of SiC abrasive paper, from P120 to P2000 followed by polishing with

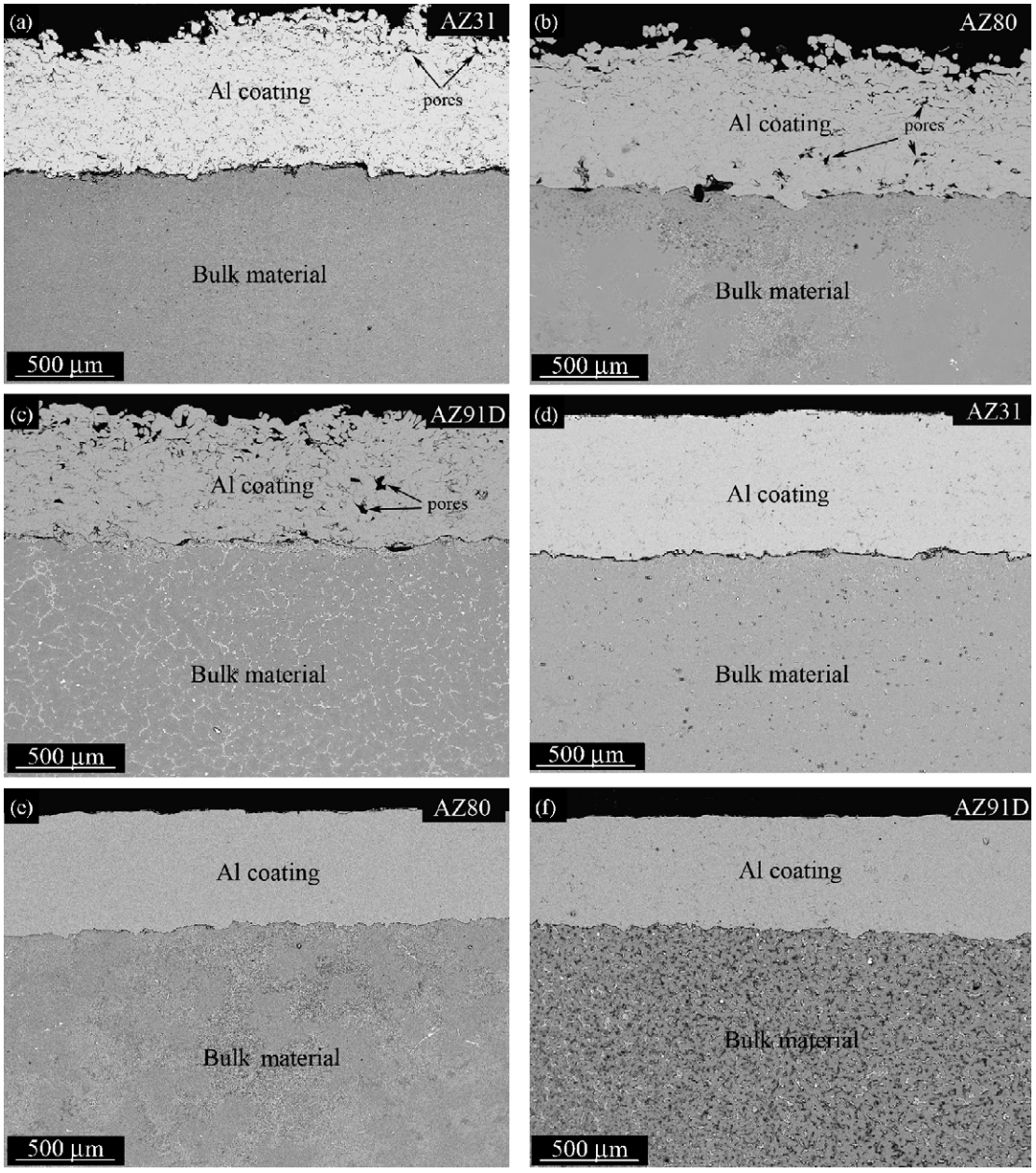

Fig. 1. Backscattered scanning electron micrographs of the cross-sections of (a–c) Al-TS and (d–f) Al-TS + CP coatings (AZ31, AZ80 and AZ91D alloys).

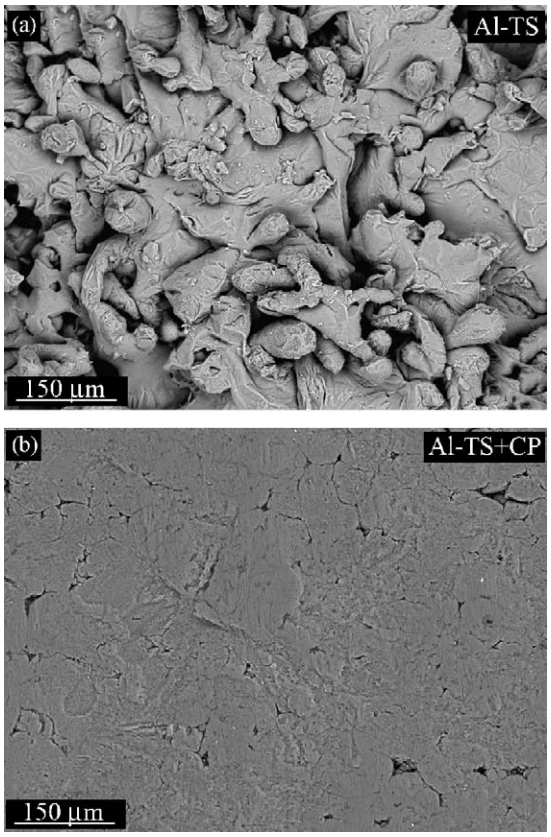

Fig. 2. Scanning electron micrographs of the surface morphology of Al-coatings on the AZ31 alloy: (a) Al-TS and (b) Al-TS + CP.

0.1 μm diamond paste. Two etching reagents were used: (a) Nital, 5 mL HNO_3 + 95 mL ethanol, to reveal the constituents and general microstructure of Mg, AZ80 and AZ91D materials and (b) Vilella reagent, 0.6 g picric acid + 10 mL ethanol + 90 mL H_2O, to reveal the grain boundaries in the AZ31 alloy. The constituents were examined by scanning electron microscopy (SEM) using a JEOL JSM-6400 microscope equipped with Oxford Link energy dispersive X-ray (EDX) microanalysis hardware. Low-angle X-ray diffraction (XRD) studies were carried out by using a Philips X'Pert diffractometer (K_αCu = 1.54056 Å).

2.4. Gravimetric measurements

Gravimetric measurements were performed using rectangular (Mg and AZ31) and cylindrical (AZ80 and AZ91D) specimens of working area ~15 cm^2 immersed in 3.5 wt.% NaCl solution at room temperature (pH 5.6, 22 °C). Prior to the tests, specimens were measured and weighed. Once the test was finished for each immersion time, the samples were extracted, rinsed with isopropyl alcohol, dried in hot air, and then weighed again in order to calculate the mass gain per unit surface area. Corrosion rate was calculated from the mass gain per unit of surface area, determined from the expression $(M_i - M_f)/A$, where M_i is the initial mass, M_f the final mass and A the exposed surface area.

2.5. Electrochemical measurements

DC electrochemical measurements were performed using an AUTOLAB-PGSTAT 30 computer-controlled potentiostat and a conventional three-electrode cell, employing a graphite counter electrode and a silver–silver chloride reference electrode (SSE) with a potential of 0.197 V with respect to the standard hydrogen electrode (SHE). The solution concentration inside the reference electrode compartment was 3 M KCl. The working electrode with 2 cm^2 of exposed area was the test material and the solution was naturally aerated 3.5 wt.% NaCl solution at room temperature (22 °C). Immersion times were up to 7 days. Cyclic polarization measurements were undertaken at a scan rate of 0.3 mV s^{-1}, from −100 mV to +400 mV with respect to the corrosion potential (E_{corr}). The potential was scanned back when the polarization curve reached the anodic current density of 5 mA cm^{-2}. In order to obtain additional information, pH changes of the test solution as a function of the immersion time were recorded during the experiments using a standard pH-meter.

Table 2
Kinetic laws of the materials immersed in 3.5 wt.% NaCl solution.

Material		Kinetic law: $y = bt$ [y (mg/cm^2); t (h)]
Mg (99%)	Un-coated	$y = -1303 \times 10^{-2} t$ $(0 \le t \le 16)$ $(r^2 = 0.99)$
	TS	$y = 906 \times 10^{-2} t$ $(0 \le t \le 16)$ $(r^2 = 0.97)$
		$y = -729 \times 10^{-2} t$ $(18 \le t \le 50)$ $(r^2 = 0.96)$
	TS + CP	$y = 1.20 \times 10^{-2} t$ $(0 \le t \le 240)$ $(r^2 = 0.97)$
AZ31	Un-coated	$y = -23.10 \times 10^{-2} t$ $(0 \le t \le 240)$ $(r^2 = 0.99)$
	TS	$y = 24.60 \times 10^{-2} t$ $(0 \le t \le 240)$ $(r^2 = 0.99)$
	TS + CP	$y = 1.01 \times 10^{-2} t$ $(0 \le t \le 240)$ $(r^2 = 0.97)$
AZ80	Un-coated	$y = -0.31 \times 10^{-2} t$ $(0 \le t \le 240)$ $(r^2 = 0.98)$
	TS	$y = 5.59 \times 10^{-2} t$ $(0 \le t \le 240)$ $(r^2 = 0.98)$
	TS + CP	$y = 1.22 \times 10^{-2} t$ $(0 \le t \le 240)$ $(r^2 = 0.96)$
AZ91	Un-coated	$y = -0.37 \times 10^{-2} t$ $(0 \le t \le 240)$ $(r^2 = 0.98)$
	TS	$y = 6.97 \times 10^{-2} t$ $(0 \le t \le 240)$ $(r^2 = 0.98)$
	TS + CP	$y = 1.70 \times 10^{-2} t$ $(0 \le t \le 240)$ $(r^2 = 0.96)$

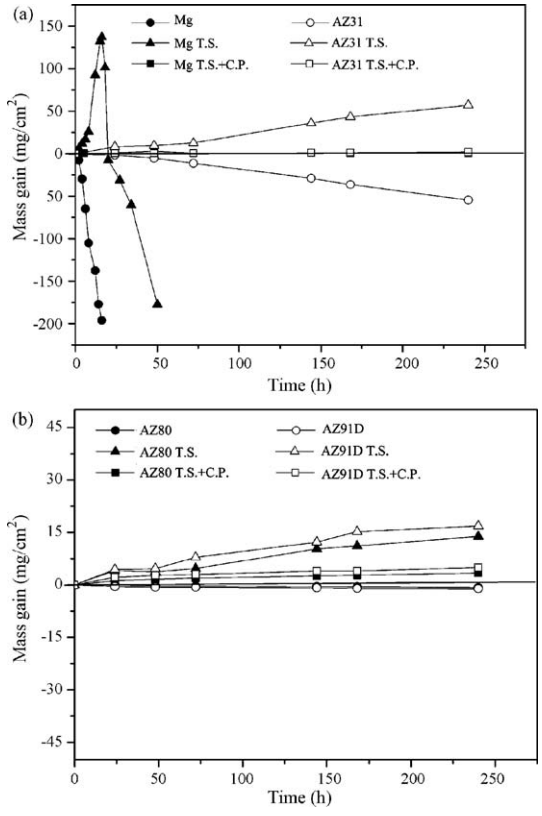

Fig. 3. Mass changes versus time after immersion in 3.5 wt.% NaCl solution at 22 °C: (a) Mg metal and AZ31 and (b) AZ80 and AZ91D specimens.

2.6. Characterization of corrosion products

The corroded surfaces were examined using SEM, EDX and low-angle XRD in order to determine the composition, morphology and evolution of the corrosion products formed on the surface.

3. Results and discussion

3.1. Microstructural characterization

Fig. 1a–f shows the backscattered scanning electron (BSE) micrographs of the cross-sections of as-sprayed (Al-TS) and cold-pressed Al-coatings (Al-TS + CP). For all the investigated magnesium alloys, the Al-TS coatings revealed an average thickness of 600 ± 15 μm with a very rough surface, interconnected pores randomly distributed within the layer and poor bonding at the substrate/coating interface (Fig. 1a–c). The latter presented some roughness due to the sand blasting pre-treatment.

The cold-pressing post-treatment under 32 MPa at room temperature produced smoother surfaces and more homogeneous and compact Al-coatings with a thickness of 500 ± 5 μm (Figs. 1d–f and 2). This corresponded to a thickness reduction by at least 17% compared with the as-sprayed coatings. SEM examination also revealed the absence of cracks/pores at the substrate/coating interface. Thus, the applied post-treatment produced a significant reduction of the porosity level and improved the bonding of the coating to the substrate. Unlike hot-pressing post-treatments [16] there was no evidence of deformation microstructures of the substrates or inter-diffusion or compound layers between the Al-coatings and the magnesium substrates.

3.2. Gravimetric results

Fig. 3 shows the mass changes of the tested materials after immersion in 3.5 wt.% NaCl solution for several times up to 10 days. The untreated materials gradually dissolved in the test solution with mass losses following approximately linear kinetics. Commercially pure Mg was completely dissolved after 16 h of immersion in the test solution, whereas magnesium/aluminium alloys revealed lower mass losses. The AZ80 and AZ91D magnesium alloys revealed a significant higher corrosion resistance than that of Mg and AZ31 materials [25,26].

The Al-TS coatings changed the corrosion behaviour of all investigated materials, which, in general, exhibited mass gain during the immersion test. Possibly, the interconnected pores in these coatings facilitated the penetration of chloride ions with the subsequent corrosion attack and formation of aluminium and magnesium corrosion products. Thus, the Al-TS coatings provided low corrosion protection to the magnesium substrates; for instance, pure Mg was completely dissolved after 2 days of immersion. On the other hand, the cold-pressed Al-coatings (Al-TS + CP) revealed significantly lower values of mass gain suggesting that the improved corrosion performance of the Al-TS + CP coatings was directly associated with the elimination of interconnected pores within the layers after the cold-pressing post-treatment.

The kinetic laws calculated from the experimental data in Fig. 3 are shown in Table 2. In each case, they were approximated by a linear equation $y = b \cdot t$, where "y" coordinate represents the mass gain in mg cm^{-2} and "t" is the immersion time in hours. Negative values of the kinetic constant (b) were attributed to the dissolution of the magnesium matrix, whereas positive values were associated with the formation of corrosion products. Increasing amounts of aluminium in the bulk composition of the magnesium alloys reduced the corrosion rate for both untreated substrates and Al-TS coated specimens. In the case of Al-TS + CP coatings, all the substrates presented lower corrosion rates ($\sim 1.5 \times 10^{-2}$ mg cm^{-2} h^{-1}) compared with the Al-TS coatings ($>6.0 \times 10^{-2}$ mg cm^{-2} h^{-1}). Besides, the corrosion rates were very similar regardless of the composition of

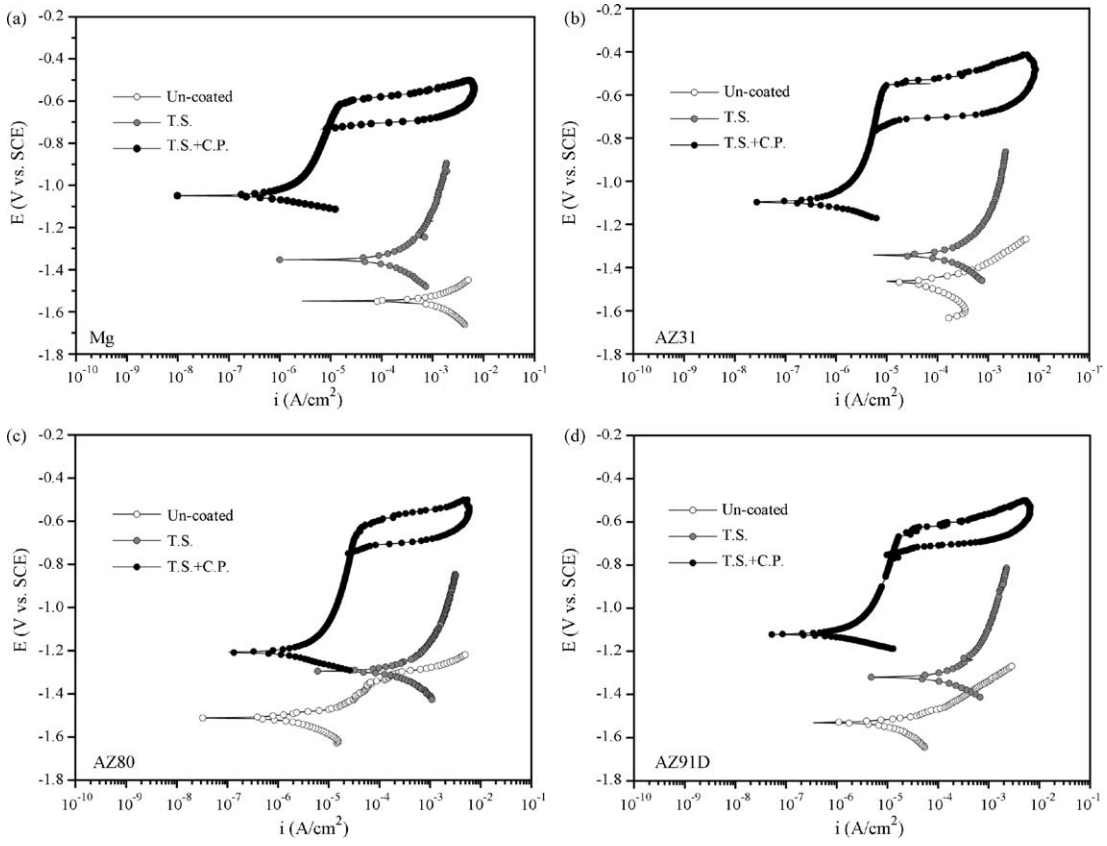

Fig. 4. Anodic and cyclic polarization curves in 3.5 wt.% NaCl solution for 1 h: (a) Mg, (b) AZ31, (c) AZ80 and (d) AZ91D specimens.

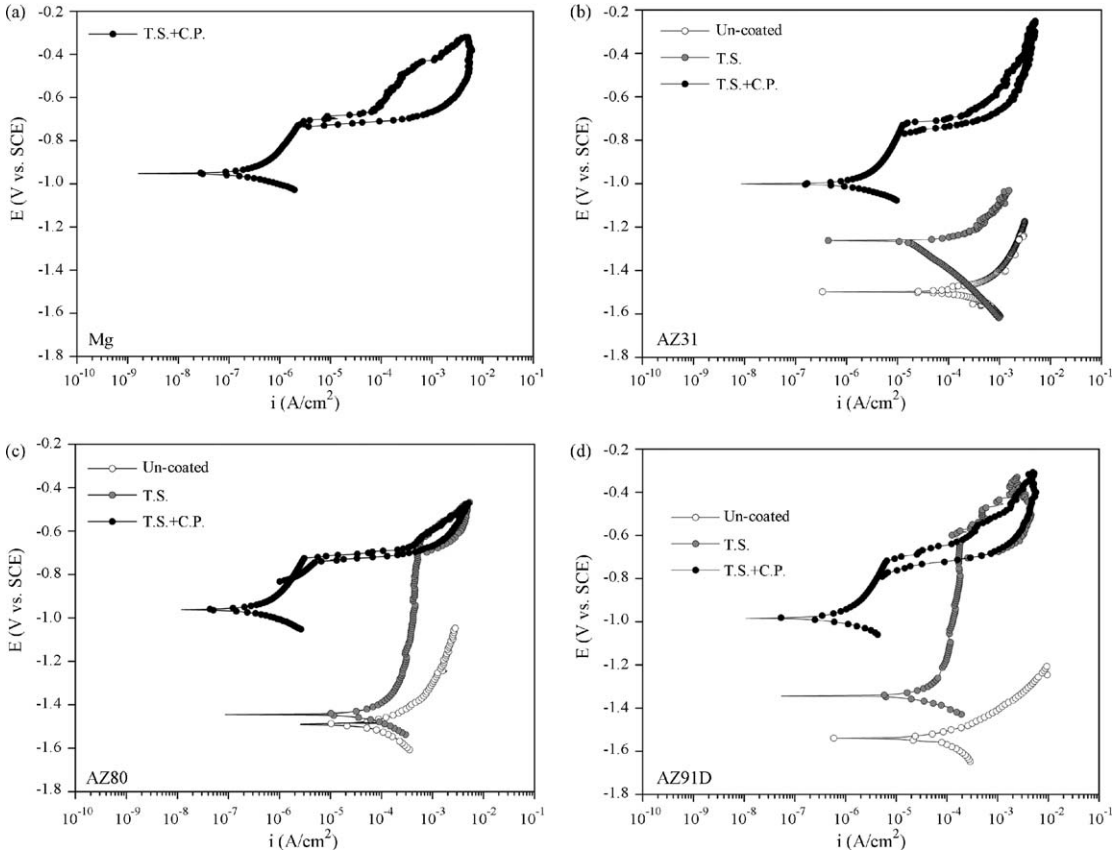

Fig. 5. Anodic and cyclic polarization curves in 3.5 wt.% NaCl solution for 7 days: (a) Mg, (b) AZ31, (c) AZ80 and (d) AZ91D specimens.

the substrate, suggesting a lower porosity degree and hampered access of electrolyte species towards the magnesium substrate.

3.3. Electrochemical results

Fig. 4 shows the anodic and cyclic polarization curves of all tested specimens after immersion in 3.5 wt.% NaCl for 1 h. Compared with the untreated materials ($E_{corr} = -1.5\ V_{SSE}$), E_{corr} shifted towards the more noble values after the deposition of Al-TS ($E_{corr} = -1.3\ V_{SSE}$) and Al-TS + CP coatings ($E_{corr} = -1.1/-1.2\ V_{SSE}$) due to the higher nobility of aluminium than that of magnesium.

The corrosion current density, i_{corr}, of as-received alloys decreased with higher aluminium content in the composition of the alloys, from $\sim 4 \times 10^{-3}$ A cm^{-2} for pure Mg, to 2×10^{-5} A cm^{-2} for magnesium alloys containing 8–9 wt.% aluminium [25,26]. The i_{corr} values of Al-TS coatings were similar or even higher in the case of AZ80 and AZ91D alloys. The latter suggested penetration of the electrolyte through the interconnected pores in the Al-TS coatings and galvanic acceleration of the corrosion of the magnesium substrates. The application of a cold-pressing post-treatment greatly enhanced the corrosion performance of Al-sprayed coatings in 3.5 wt.% NaCl solution. Thus, for the Al-TS + CP coatings the i_{corr} values were around 10^{-6} A cm^{-2} and a passive range of 0.5 V was observed between the E_{corr} and the pitting potential at approximately −0.60 V. The results obtained for the Al-TS + CP coatings were similar to those reported for aluminium thermal spray coatings on other magnesium alloys. For instance, Wei et al. [18] and Chiu et al. [19] reported i_{corr} values in the same range for hot-pressed arc-spray aluminium coatings on the AZ31 alloy immersed in 3.5 wt.% NaCl solution.

Fig. 5 discloses the evolution of the electrochemical behaviour of each material after 7 days of immersion in the saline solution. The high dissolution rate observed for pure magnesium before and after the deposition of the Al-TS coating limited its electrochemical study to the first stages of immersion in 3.5 wt.% NaCl. In general, for long immersion times, the polarization curves of untreated materials shifted toward greater current densities, suggesting that the formation of corrosion products did not impede the progression of the corrosion attack. On the other hand, the polarization curves of the Al-TS + CP coatings practically remained unchanged during the experiments, indicating a steady performance of these coatings.

The comparison of the polarization resistance (R_p) values, determined from the electrochemical tests, revealed values of up to $\sim 10^4\ \Omega$ cm^2 for the Al-TS + CP coatings after immersion in 3.5 wt.% NaCl for 1 h, which were higher than those of un-treated specimens and Al-TS coatings by one to three orders of magnitude (Table 3). In general, the R_p values of magnesium alloys with Al-

Table 3
Variation of R_p as a function of the immersion time in 3.5 wt.% NaCl solution.

Material		R_p (kΩ cm^2)			
		1 h	1 day	3 days	7 days
Mg (99%)	Un-coated	0.02	0.03	–	–
	TS	0.22	0.21	0.14	–
	TS + CP	16.3	26.4	108	110
AZ31	Un-coated	0.35	0.32	0.24	0.11
	TS	0.17	0.21	0.19	0.28
	TS + CP	16.3	64.8	119	120
AZ80	Un-coated	5.30	2.96	2.12	0.30
	TS	0.18	0.24	0.34	0.38
	TS + CP	14.0	53.4	60.2	90.0
AZ91	Un-coated	1.30	0.88	0.31	0.16
	TS	0.18	0.29	0.41	0.52
	TS + CP	15.0	50.1	72.8	92.0

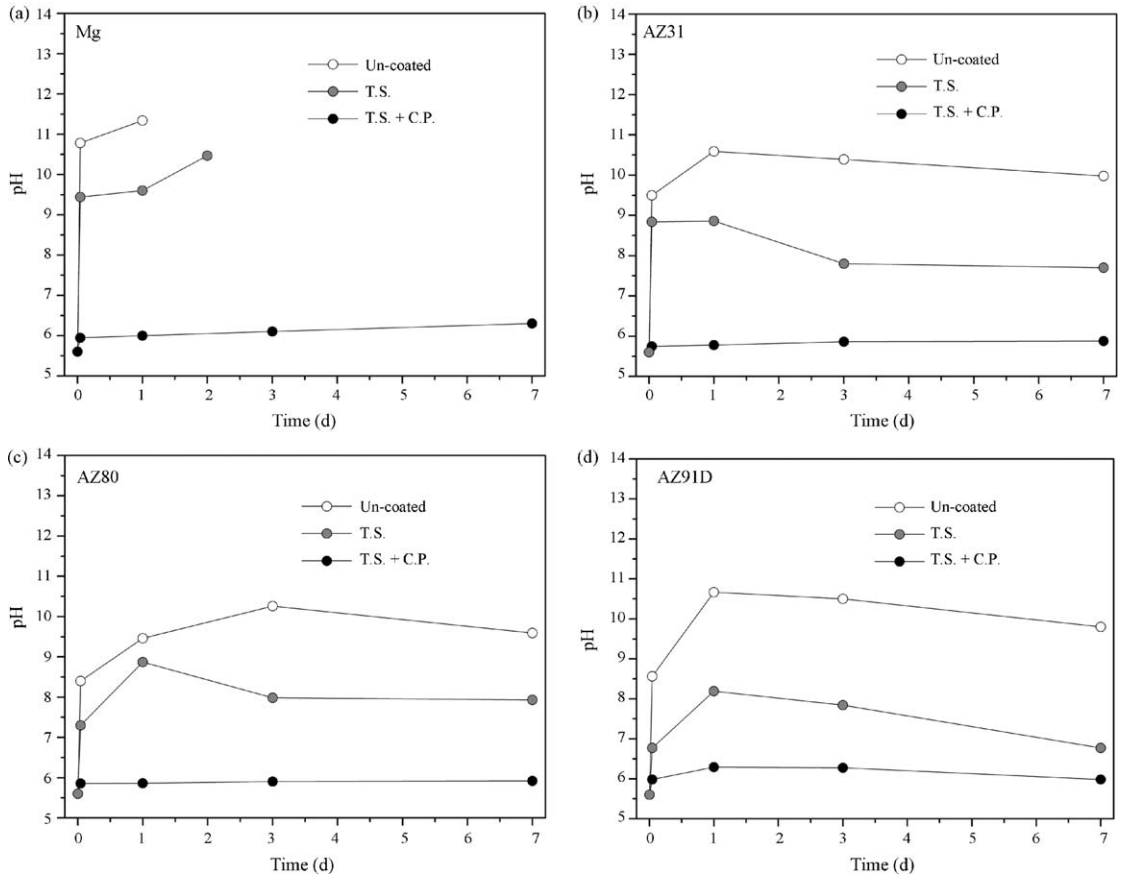

Fig. 6. Evolution of the pH values of the test solution for immersion times up to 7 days for all specimens tested: (a) Mg, (b) AZ31, (c) AZ80 and (d) AZ91D.

coatings increased with the immersion time, especially in the case of Al-TS + CP coatings. This was possibly related to the nucleation and growth of a slightly protective layer of aluminium-rich corrosion products over the coating surface that offered additional electrochemical resistance.

3.4. pH measurements

It is known, that an oxide film mainly consisting of magnesium hydroxide or brucite forms on the surface of magnesium when it is exposed to the atmosphere or aqueous solutions. This film is stable in the basic range of pH values, but in the presence of chloride anions the surface film breaks down and magnesium appears unprotected. Although corrosion mechanism of magnesium needs further investigation, it is generally reported that the following reactions take place in aqueous environments:

$$Mg(s) \rightarrow Mg^{2+}(aq) + 2e^{-} \quad \text{(anodic reaction)} \tag{1}$$

$$2H_2O + 2e^{-} \rightarrow H_2 + 2OH^{-}(aq) \quad \text{(cathodic reaction)} \tag{2}$$

$$Mg^{2+}(aq) + 2OH^{-}(aq) \rightarrow Mg(OH)_2(s) \quad \text{(corrosion product)} \tag{3}$$

Thus, pH values of the test solution increase along with the cathodic reaction due to the formation of OH^- and, therefore, for a given immersion time higher pH values suggest higher corrosion rate of magnesium. According to this, pH values can be measured in order to follow the evolution of magnesium alloys immersed in 3.5 wt.% NaCl (Fig. 6). These measurements were carried out with duplicate specimens of 15 cm^2 immersed in 500 ml of test solution at 22 °C.

At the early stages of the corrosion process (1 h), all un-coated magnesium alloys revealed a sudden and sharp increase of the pH ($pH > 10$), which was attributed to the corrosion attack produced when the aggressive solution reacts with the fresh magnesium surfaces. For increasing immersion times, the pH values remained practically constant or slightly decreased due to the saturation of the solution with $Mg(OH)_2$ and some acidification due to increasing concentrations of atmospheric carbon dioxide in the test solution. Likewise, a rapid increase of the pH values was observed for the Al-TS and Al-TS + CP coatings, although less evident for the cold-pressed coatings. However, the pH values remained lower than those of un-coated magnesium materials, indicating that the deposited Al-coatings, especially the Al-TS + CP coatings, reduced the participation of magnesium in the corrosion mechanism of the investigated materials.

3.5. Characterization of corrosion products

The scanning electron micrograph of the cross-section of the AZ31 alloy after immersion in the aggressive solution for 10 days revealed a thick corrosion layer of irregular thickness between 300 and 500 μm, probably consisting of magnesium oxides/hydroxides (Fig. 7a) [25,26]. On the other hand, the Al-coated specimens revealed less corrosion damage of the magnesium substrate and formation of aluminium corrosion products as a result of corrosion of the Al-coatings (Fig. 7b and c). For the Al-TS specimens, the SEM study at higher magnification revealed a non-uniform attack with a ~15 μm-thick aluminium-rich corrosion layer in the outer coating surface and corrosion products throughout the cavities within the coating. This indicated that the aggressive solution readily penetrates towards the bulk material facilitating the galvanic acceleration of the corrosion of the magnesium substrate (Fig. 8). The Al-TS + CP coatings revealed a more homogeneous and thinner corrosion layer (~4 μm) compared with the Al-TS coatings, and the

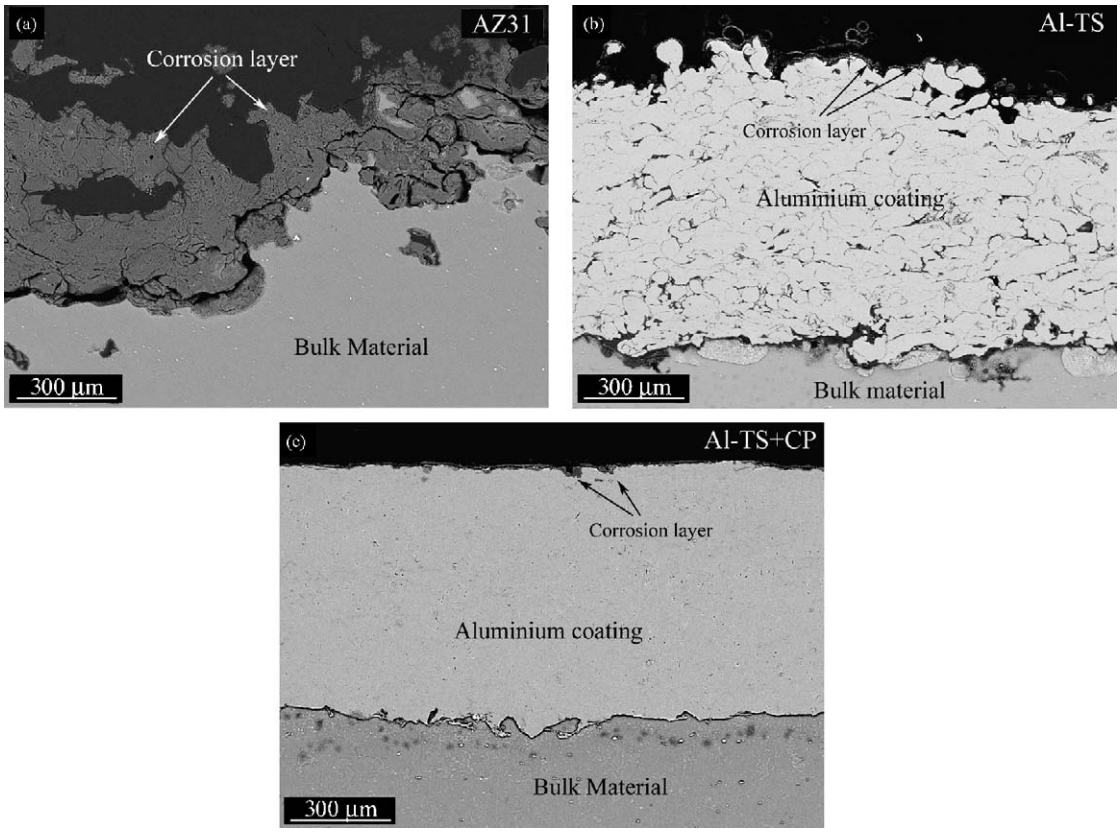

Fig. 7. Backscattered scanning electron micrographs of the cross-sections of the AZ31 specimens after immersion in 3.5 wt.% NaCl for 10 days: (a) un-coated, (b) Al-TS and (c) Al-TS + CP.

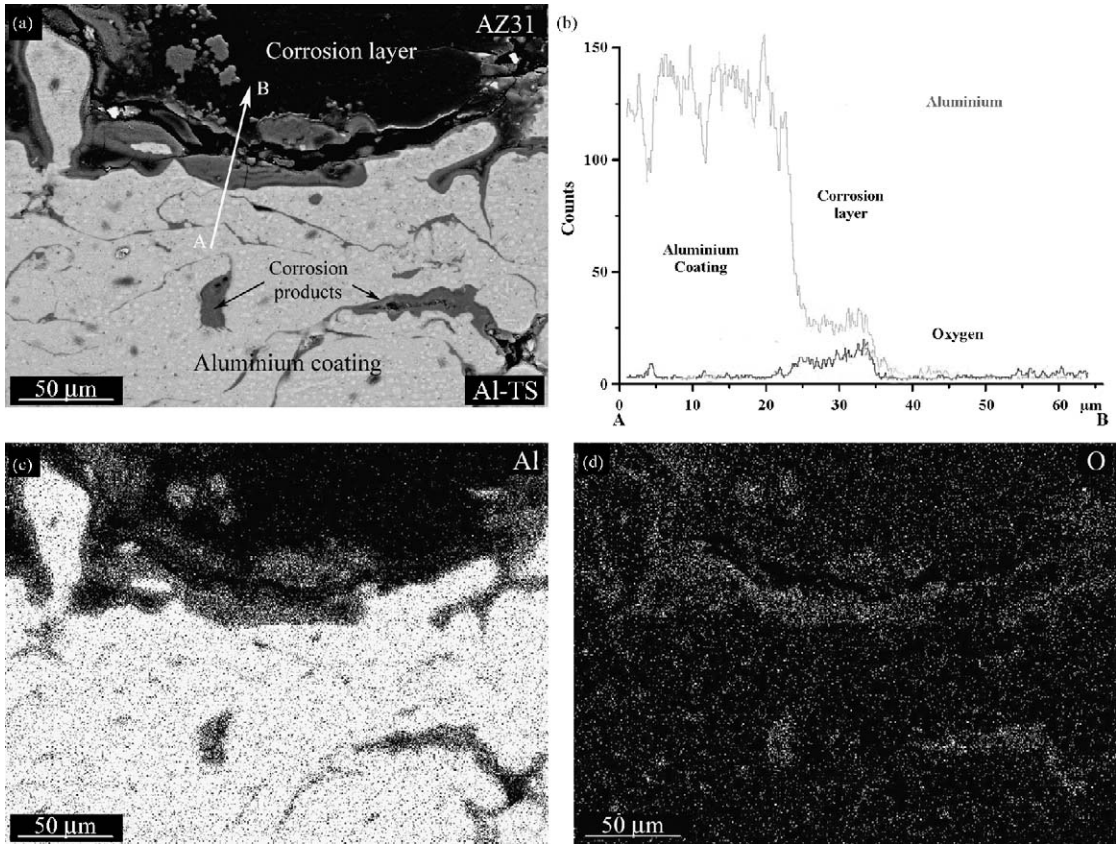

Fig. 8. (a) SEM detail of the cross-section of the AZ31 Al-TS specimen after immersion in 3.5 wt.% NaCl for 10 days; (b) profile line analysis at the coating surface; (c) Al and (d) O X-ray elemental maps.

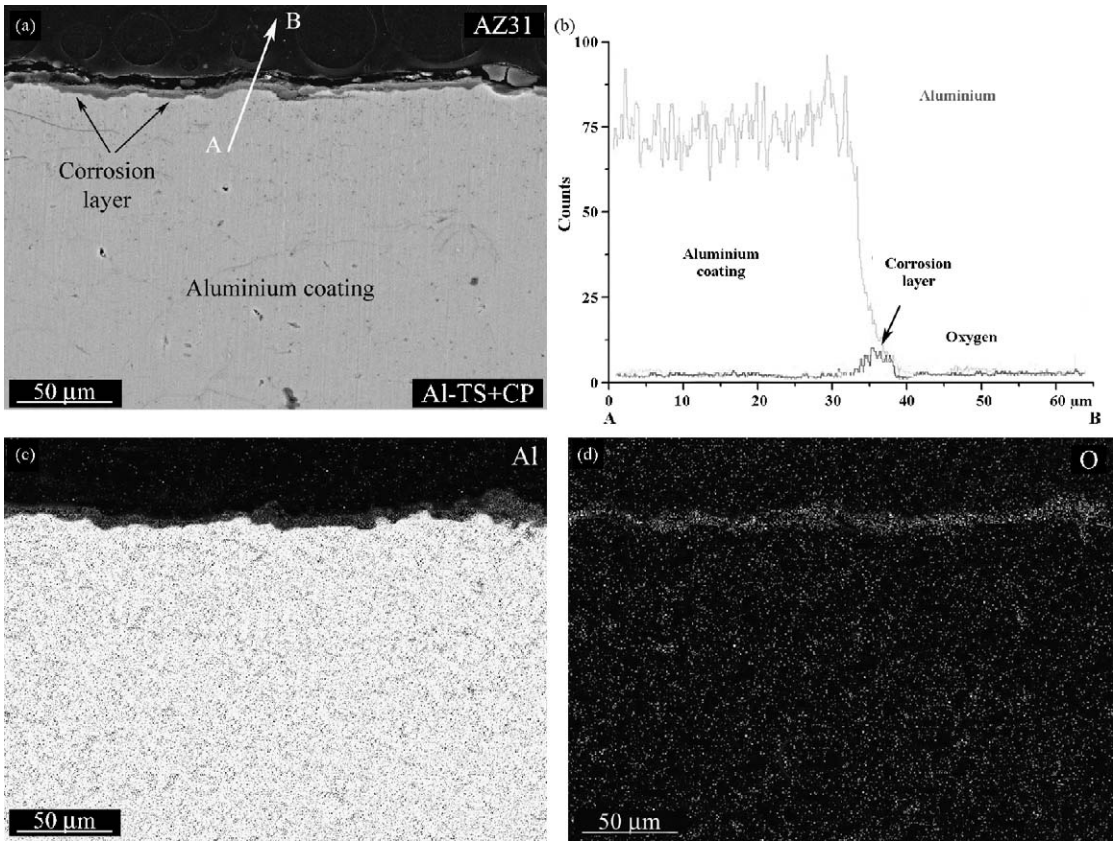

Fig. 9. (a) Backscattered scanning electron micrograph of the cross-section of the AZ31 Al-TS + CP specimen after immersion in 3.5 wt.% NaCl for 10 days; (b) profile line analysis at the coating surface; (c) Al and (d) O X-ray elemental maps.

absence of corrosion products in the inner regions of the coating (Fig. 9). According to the electrochemical results this layer provided some corrosion protection with increasing immersion times in 3.5 wt.% NaCl.

The examination of the cross-sections of the AZ80 and AZ91D alloys with Al-TS + CP coatings after immersion in the test solution for 10 days (Fig. 10) indicated that these specimens followed a similar corrosion mechanism to that observed for the AZ31 alloy. For all the Al-coatings there was no evidence of delamination attack at the coating/bulk material interface. Thus, according to the gravimetric and electrochemical results and SEM observation, the corrosion behaviour of the Al-TS + CP specimens was unaffected by the nature of the magnesium substrate, indicating that the cold-pressing post-treatment is an effective process to reduce the corrosion susceptibility of magnesium alloys with aluminium thermal spray coatings.

Fig. 11 discloses the average thickness of the corrosion layer determined from SEM observation of all the specimens after immersion in 3.5 wt.% NaCl solution for 10 days. The cold-pressing post-treatment reduced the thickness of the corrosion layer, compared with the untreated materials, by 40–75 times depending on the magnesium alloy. The thickness of the corrosion layer

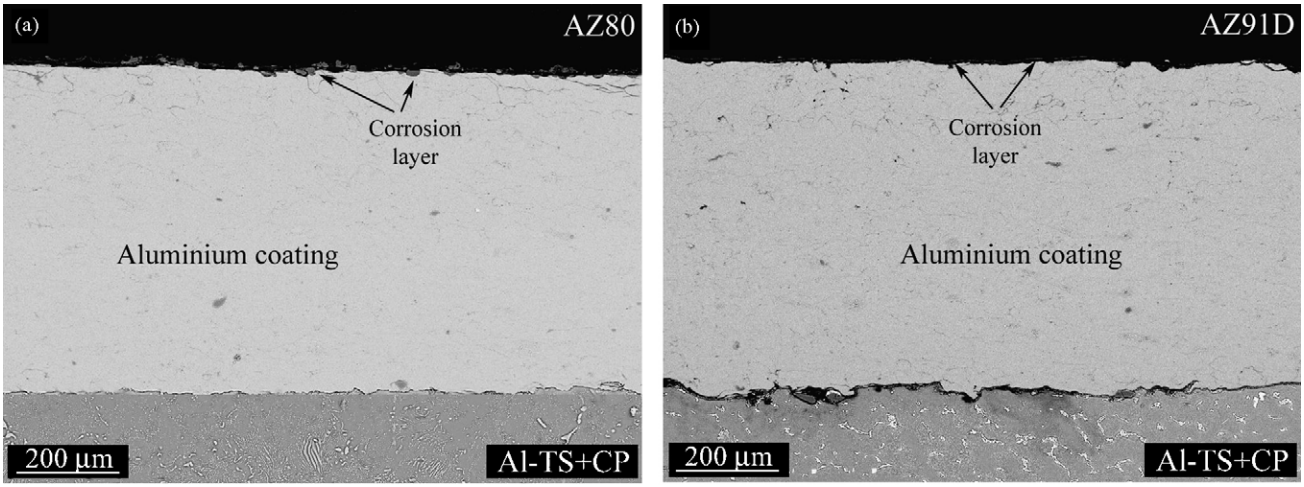

Fig. 10. Backscattered scanning electron micrographs of the cross-sections of the Al-TS + CP coatings after immersion in 3.5 wt.% NaCl for 10 days: (a) AZ80 and (b) AZ91D.

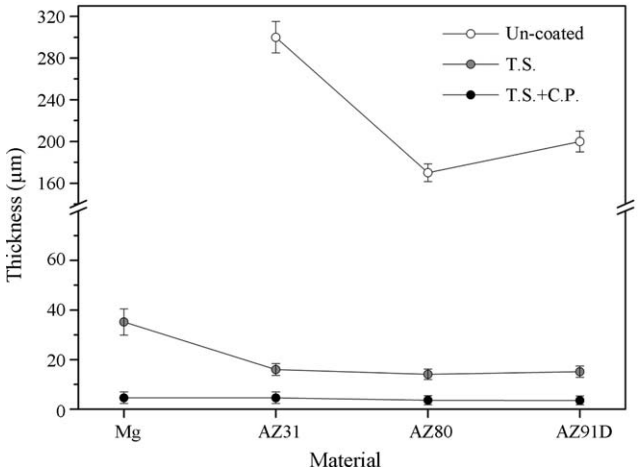

Fig. 11. Thickness values of the corrosion layer determined for all specimens tested after immersion in 3.5 wt.% NaCl for 10 days.

formed in the Al-TS specimens was also inferior to that of untreated specimens, although, in this case the corrosion products formed within the coating should be taken into consideration.

The low-angle (1°) XRD study of the corrosion layer formed on the un-coated magnesium alloys after immersion in 3.5 wt.% NaCl for 10 days revealed brucite ($Mg(OH)_2$) as the main corrosion product, which revealed higher intensity peaks for Mg and AZ31 materials due to formation of a thicker corrosion layer during the severe attack that both materials disclosed (Fig. 12a). On the other hand, the corrosion layer formed on the Al-TS and Al-TS + CP specimens consisted of bayerite (β-$Al_2O_3{\cdot}3H_2O$), with lower intensity peaks for the Al-TS specimens (Fig. 12b and c). This may be attributed to the higher surface roughness and non-uniformity of the corrosion attack that these coatings exhibited.

4. Conclusions

1. The investigated magnesium alloys revealed severe corrosion attack in 3.5 wt.% NaCl solution characterized by the nucleation and growth of an irregular and low protective corrosion layer of $Mg(OH)_2$.
2. The as-sprayed aluminium coatings (Al-TS) revealed a poor corrosion performance in the test solution due to their high degree of interconnected pores facilitating the penetration of aggressive species towards the bulk material. Aluminium corrosion products were observed within the cavities of the coatings. Crevice corrosion phenomena may occur within these cavities. Additionally, galvanic acceleration of the corrosion attack of the magnesium alloys was observed when the electrolyte reached the coating/substrate interface.
3. The application of a cold-pressing post-treatment resulted in more homogeneous coatings with a better bonding at the

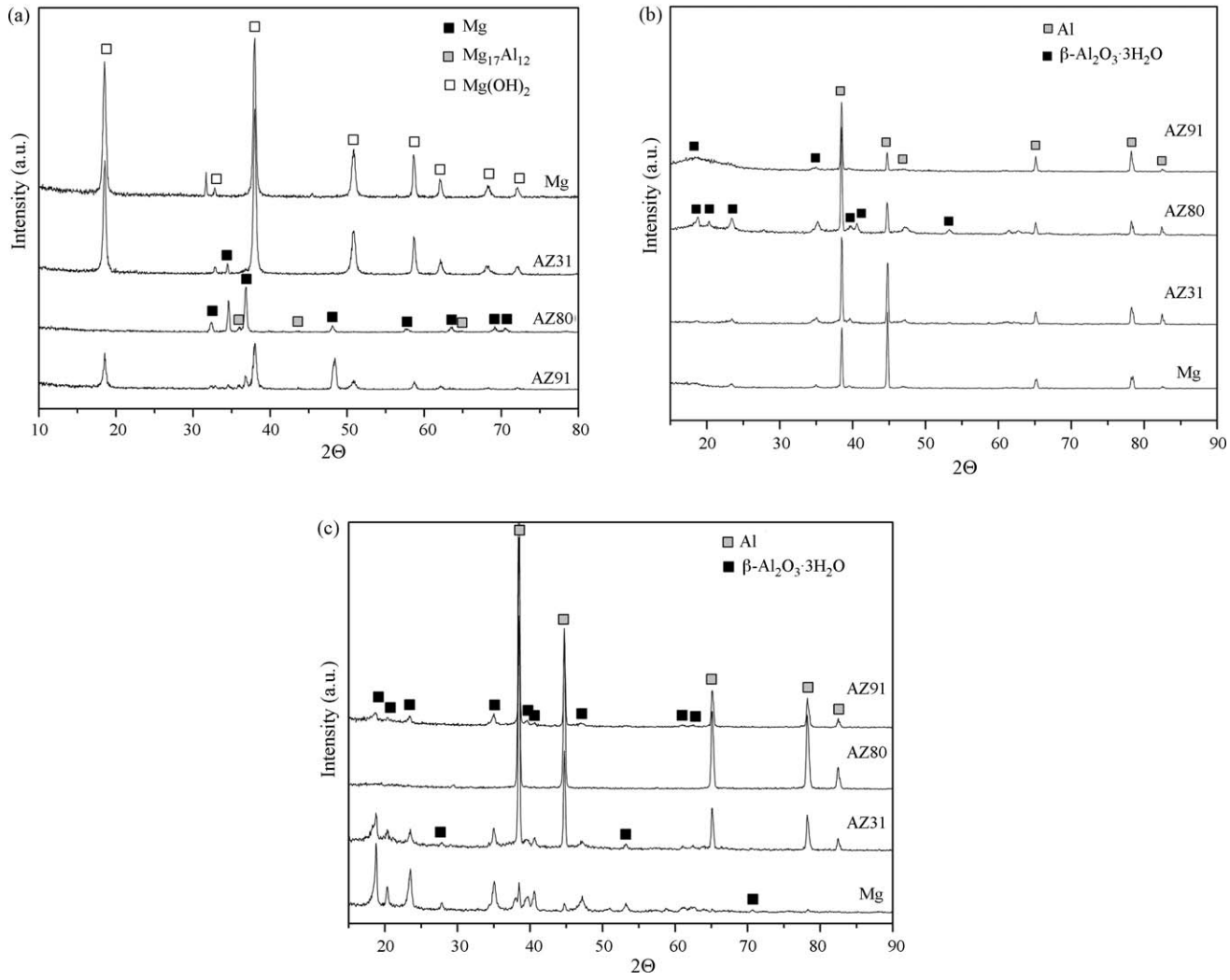

Fig. 12. Low-angle (1°) XRD study of all specimens immersed in 3.5 wt.% NaCl solution for 10 days: (a) un-coated, (b) Al-TS and (c) Al-TS + CP.

substrate/coating interface and a significant reduction of the porosity level. Accordingly, the corrosion performance of all investigated alloys was enhanced regardless of their composition or microstructure.

Acknowledgement

The authors wish to thank the MCYT for the financial support given to this work (Project MAT2006-13179-C02-01-02).

References

[1] T.J. Polmear, Light Alloys—Metallurgy of the Light Metals, second ed., Edward Arnold, London, UK, 1995.
[2] W.S. Loose, in: L.M. Pidgeon, J.C. Mathes, N.E. Woldmen (Eds.), Corrosion and Protection of Magnesium, Metals Handbook, ASM International, Materials Park, OH, USA, 1946, p. 173.
[3] R. Ambat, N.N. Aung, W. Zhou, J. Appl. Electrochem. 30 (2000) 865.
[4] M. Walter, in: K.U. Kainer (Ed.), Proc. of the 6th Int. Conf. Magnesium Alloys and Their Applications, Wiley-VCH Verlag, Wolfsburg, Germany, 2003, p. 529.
[5] H. Umehara, T. Okada, Y. Togawa, Report of Industrial Products Research Institute, No. 125, 1992, p. 43.
[6] J.E. Gray-Munro, B. Luan, L. Huntington, Appl. Surf. Sci. 254 (2008) 2871.
[7] Y. Gao, X. Xu, Z. Yan, G. Xin, Surf. Coat. Technol. 154 (2002) 189.
[8] R.S.C. Paredes, S.C. Amico, A.S.C.M. d'Oliveira, Surf. Coat. Technol. 200 (2006) 3049.
[9] W.Y. Li, C. Zhang, X. Guo, G.J. Li, H. Liao, C. Coddet, Appl. Surf. Sci. 254 (2007) 517.
[10] G. Barbezat, Surf. Coat. Technol. 200 (2005) 1990.
[11] G. Barbezat, Surf. Coat. Technol. 201 (2006) 2028.
[12] M. Parco, L. Zhao, J. Zwick, K. Bobzin, E. Lugscheider, Surf. Coat. Technol. 201 (2007) 6290.
[13] E. Lugscheider, M. Parco, K.U. Kainer, N. Hort, in: K.U. Kainer (Ed.), Proc. of the 6th Int. Conf. Magnesium Alloys and Their Applications, Wiley-VCH Verlag, Wolfsburg, Germany, 2003, p. 860.
[14] Fr.-W. Bach, K. Möhwald, Z. Babiak, J. Prehm, L. Engl, E. Lugscheider, M. Parco, R. Dicks, in: M. Geiger, K.-D. Bouzakis, B. Denkena, H.-K. Tönshoff, Fr.-W. Bach, U. Popp (Eds.), Proc. of the 47th International Conference THE Coatings, Bamberg, Meisenbach, Erlangen, Germany, April 5–7, (2004), p. 425.
[15] Fr.-W. Bach, K. Möhwald, L. Engl, E. Lugscheider, M. Parco, K. Seemann, in: E. Lugscheider (Ed.), Proc. of the International Thermal Spray Conference ITSC 2005, DVS-Verlag, Dusseldorf, Basel, Germany, 2005.
[16] H. Pokhmurska, B. Wielage, T. Lampke, T. Grund, M. Student, N. Chervinska, Surf. Coat. Technol. 202 (2008) 4515.
[17] M. Parco, L. Zhao, J. Zwick, K. Bobzin, E. Lugscheider, Surf. Coat. Technol. 201 (2006) 3269.
[18] Z. Wei, L. Liu, W. Ding, Mater. Sci. Forum 488–489 (2005) 685.
[19] L.H. Chiu, H.A. Lin, C.C. Chen, C.F. Yang, C.H. Chang, J.C. Wu, Mater. Sci. Forum 419–422 (2003) 909.
[20] J. Zhang, Y. Wang, R.C. Zeng, W.J. Huang, Mater. Sci. Forum 546–549 (2007) 529.
[21] S. Ignat, P. Sallamand, D. Grevey, M. Lambertin, Appl. Surf. Sci. 225 (2004) 124.
[22] Ch. Christoglou, N. Voudouris, G.N. Angelopoulos, M. Pant, W. Dahl, Surf. Coat. Technol. 184 (2004) 149.
[23] I. Shigematsu, M. Nakamura, N. Saitou, K. Shimojima, J. Mater. Sci. Lett. 19 (2000) 473.
[24] L. Zhu, G. Song, Surf. Coat. Technol. 200 (2006) 2834.
[25] A. Pardo, M.C. Merino, A.E. Coy, R. Arrabal, F. Viejo, E. Matykina, Corros. Sci. 50 (2008) 823.
[26] A. Pardo, M.C. Merino, A.E. Coy, F. Viejo, R. Arrabal, S. Feliú Jr., Electrochim. Acta 53 (2008) 7890.